

Effects of volume and electronic concentration on the $\text{Ce}(\text{Pd}_{1-x}\text{M}_x)$ compounds ($M = \text{Ni}, \text{Rh}, \text{and Ag}$)

J. G. Sereni

Comisión Nacional de Energía Atómica, Centro Atómico Bariloche, 8400 S.C. de Bariloche, Argentina

E. Beaurepaire and J. P. Kappler

*Institut de Physique et Chimie des Matériaux de Strasbourg—Groupe d'Etude des Matériaux Métalliques,
4 rue Blaise Pascal, 67070 Strasbourg, France*

(Received 23 September 1992; revised manuscript received 1 March 1993)

High-field-magnetization, magnetic-susceptibility, specific-heat, electrical-resistivity, lattice-parameter, L_{III} x-ray absorption spectroscopy, and x-ray-absorption near-edge spectroscopy measurements are discussed for $\text{Ce}(\text{Pd}_{1-x}\text{M}_x)$ ($M = \text{Ni}, \text{Rh}, \text{and Ag}$) pseudoternary alloys. The Pd substitution by a holelike metal (Ni and Rh) induces the demagnetization of the Ce atom by two different mechanisms: electronic concentration variation (ΔZ , for $M = \text{Rh}$) and volume reduction (ΔV , for $M = \text{Ni}$). The Pd substitution by an electronlike metal (Ag) induces drastic changes in the magnetic structure with only a 2 at. % impurity. The experimental results indicate: (i) a continuous transformation from a ferromagnetic (F) to a nonmagnetic (NM) ground state induced by the ΔZ variation and (ii) a drastic transformation from F to NM, by the ΔV change at a certain critical concentration. The ferromagnetic-to-antiferromagnetic transition induced by Ag is described as due to the variation of the charge screening at the nonmagnetic site.

I. INTRODUCTION

The competition between the quenching of the local magnetic moments and the intersite magnetic interaction in Ce compounds has attracted the interest of experimental and theoretical researchers for more than a decade.¹⁻³ It was well established that the two mechanisms compete in the formation of the ground state with their respective energy scales: $k_B T_K$ (T_K known as the Kondo temperature) and $K_B T_R$ [identified with the Ruderman-Kittel-Kasuya-Yosida (RKKY) interaction]. Both characteristic temperatures can be expressed in terms of the $|\delta J|$ parameter (where δ is the density of the conduction states at the Fermi energy and J the exchange interaction). Their respective functional dependencies are given by $T_K \sim \exp(-1/|\delta J|)$ and $T_R \sim |\delta J|^2$. As it is well known, for small values of $|\delta J|$: $T_R > T_K$ and the system tends to order magnetically (at T_0), while for large values of $|\delta J|$: $T_K > T_R$ and it becomes nonmagnetic. For intermediate values, a maximum in T_0 was predicted and observed. Here $T_0 = T_C$ (Curie) or T_N (Néel) temperature, depending on the nature of the magnetic order: ferromagnetic (F) or antiferromagnetic (AF).

The experimental results have a good qualitative description within this framework, once the strict proportionality between the theoretical parameter $|\delta J|$ and the experimental one (for example, the Ce-ligand substitution) is skipped. Though there is no way for a direct or quantitative evaluation of $|\delta J|$, its empirical correlation with the chemical potential (the experimental driving parameter) is remarkable.

Within the Ce-binary compounds, in the cases where the Ce-ligand substitution was made with an isoelectronic element [for example in $\text{Ce}(\text{Pt}, \text{Ni})$ (Ref. 4), $\text{Ce}(\text{Pd}, \text{Ni})$ (Ref. 5), or $\text{Ce}(\text{Si}, \text{Ge})_2$ (Ref. 6)], maxima in T_0 were ob-

served. Here, the main effect is the change in the cell volume ΔV , as in CeAg under pressure where also a maximum in T_0 is observed at $P = 0.7$ GPa.⁷ However, when the substitution was made with an element of similar volume but different electronic concentration (ΔZ) [for example in $\text{Ce}(\text{Pd}, \text{Rh})$ (Ref. 8), $\text{Ce}(\text{In}, \text{Sn})_3$ (Ref. 9), or CeSi_x ($1.8 \leq x \leq 1.9$) (Ref. 10)], T_0 decreases continuously. There is another variable to be taken into account within the last case, that is the Ce-ligand substitution by an element of different electronic character (i.e., the holelike Pd by the electronlike element Ag) such as in $\text{Ce}(\text{Pd}, \text{Ag})$,¹¹ which may change the sign of the exchange interaction though not necessarily its intensity.

From these experimental evidences the question arises whether the maximum of T_0 , observed in some Ce systems is intrinsic to the $T_K - T_R$ competition, as proposed by the theory, or not.¹² One can also ask whether the changes of the chemical potential, driven by volume (ΔV) or electronic concentration (ΔZ) are actually equivalent. In other words, starting at the same $|\delta J|$ value, should they produce the same effect?

With the aim to provide experimental information for a better understanding of these different behaviors, we have carried further measurements on the $\text{Ce}(\text{Pd}_{1-x}\text{M}_x)$ pseudoternary system, where $M = \text{Rh}, \text{Ni}, \text{and Ag}$. The stoichiometric compounds, CePd, CeNi, and CeRh and their respective alloys, crystallize with the CrB-type structure,^{5,8} while in the case of $\text{Ce}(\text{Pd}, \text{Ag})$ such a structure is kept almost up to 20% of Pd substitution by Ag. The CePd compound is a ferromagnet, with $T_C = 6.5$ K,⁵ while CeNi and CeRh show the characteristic behavior of intermediate valent systems in their respective thermal, magnetic, and structural properties.¹³ We point out that Pd and Ni can be considered isoelectronic (holelike) elements, while Rh-Pd-Ag have similar volume with

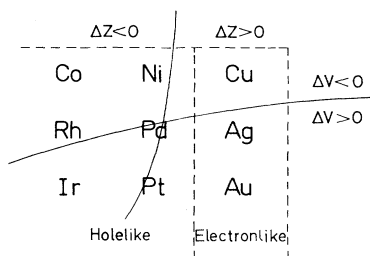


FIG. 1. ΔV and ΔZ variation illustrated from the Periodic Table of the elements.

different electronic concentration. Within the same crystalline structure and performing continuous solutions, these systems allow the study of the above described cases, providing a detailed comparison among them: (i) Pd \leftrightarrow Ni, volume effect, ΔV , (ii) Pd \leftrightarrow Rh, electronic concentration effect, ΔZ , and (iii) Pd \leftrightarrow Ag, holelike \leftrightarrow electronlike effect. These variations are represented in Fig. 1 in the Periodic Table. The comparison between the ΔV and ΔZ effects in this family of compounds is given by the fact that both systems, Ce(Pd,Ni) and Ce(Pd,Rh), have the same "matrix" compound, CePd, to which only one value of $|\delta J|$ can be attributed. In the present work, the already known thermodynamic (magnetization and specific heat), transport (electrical resistivity) and structural (lattice parameters) measurements on the mentioned compounds are compared and complemented by x-ray-absorption spectroscopy at the L_{III} -Ce edge.

II. EXPERIMENTAL AND RESULTS

The sample preparation procedure and the experimental details were discussed elsewhere.^{5,8}

A. Magnetic properties

The comparison of the ordering temperature as a function of the Pd substitution is given in Fig. 2, where a clear difference is seen depending on the nature of the substituent. Though the holelike substituents change T_C ,

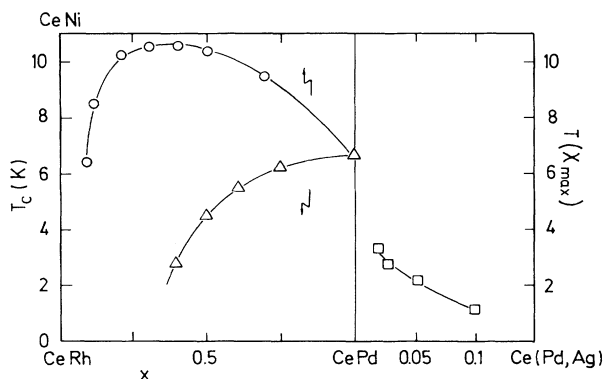


FIG. 2. Ordering temperatures of Ce(Pd,Ni) (○), Ce(Pd,Rh) (△), and Ce(Pd,Ag) (□) as a function of Pd substitution. The lines are a guide for the eye.

they do not affect the F character of the system up to $x = x(0)$, where $T_C \rightarrow 0$ [$x(0) \approx 0.92$ for Ni and ≈ 0.65 for Rh], while only 2 at. % of the electron-like Ag induces a different magnetic state with AF characteristics [i.e., a maximum in the susceptibility (χ_{\max}) as a function of T]. Only Ni substituent produces a maximum of $T_C(x)$, while Rh only depresses T_C . On the Ag side T_N has a completely different concentration dependence. The same behavior was observed by substituting Pd by Cu or Au.¹¹

In Fig. 3 we show the Curie-Weiss paramagnetic temperature, $\theta_p(x)$, dependence. Here both, Ni and Rh, substituents increase $|\theta_p|$, as expected from systems that undergo a magnetic-to-nonmagnetic transformation. The exponential increase of $\theta_p(x)$ will be discussed later. In the case of the Ag substituent, no significative changes in $\theta_p(x)$ are observed within the small x variation studied here. However, it is noteworthy that at low temperatures the 10% at. Ag sample shows a positive value of $\theta_p = 1.6$ K, suggesting a non-simple-ordered state below T_N .

Concerning the magnetization at 4.2 K, we show in Fig. 4(a) the Arrot plot, (i.e., M^2 vs H/M) of Ce(Pd,Ni), in Fig. 4(b) that of Ce(Pd,Rh) and in Fig. 4(c) that of Ce(Pd,Ag). The strong F character of Ce(Pd,Ni) is clearly shown for $x < x(0)$, in the linear M^2 vs H/M dependence to low H/M values. On the contrary, the Rh reduces the F character (which is already weakened in the CePd matrix). The experimental values are listed in Table I.

The Ag substituent slightly reduces the M_0 moment, however, the presence of a critical magnetic field at $H_C = 1.1$ T is observed. Figure 5 resumes the $M_0(x)$ dependence, extracted from the extrapolation of the linear portion in magnetic fields larger than 10 T, which reflects the F to intermediate valent (IV) ground-state (GS) transformation on the Ni and Rh-rich side, but does not indicate significative changes on the Ag one, despite of the F-AF transformation.

B. Thermal properties

A detailed report on the specific heat of the systems at hand is given in Refs. 5, 8, and 12. The comparison

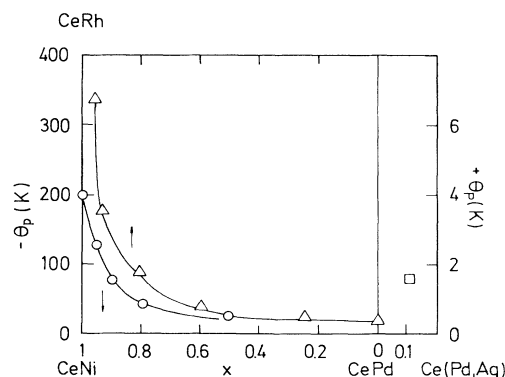


FIG. 3. Paramagnetic Curie-Weiss temperatures of Ce(Pd,Ni) (○), Ce(Pd,Rh) (△), and Ce(Pd,Ag) (□) as a function of Pd substitution. The lines are a guide for the eye.

among them is done in Fig. 6 in a $\Delta C/T$ vs T plot, where ΔC denotes the phonon subtraction. The temperature dependence of the entropy gain, $\Delta S(T)$, is shown in Fig. 7. The compounds with similar substitution, 50% of Ni and 60% of Rh, clearly show their difference in the hybridization effect. At such a concentration the Ce(Pd,Ni) system still have a magnetic GS, while the Ce(Pd,Rh) has developed a mixed valent GS. This difference can be

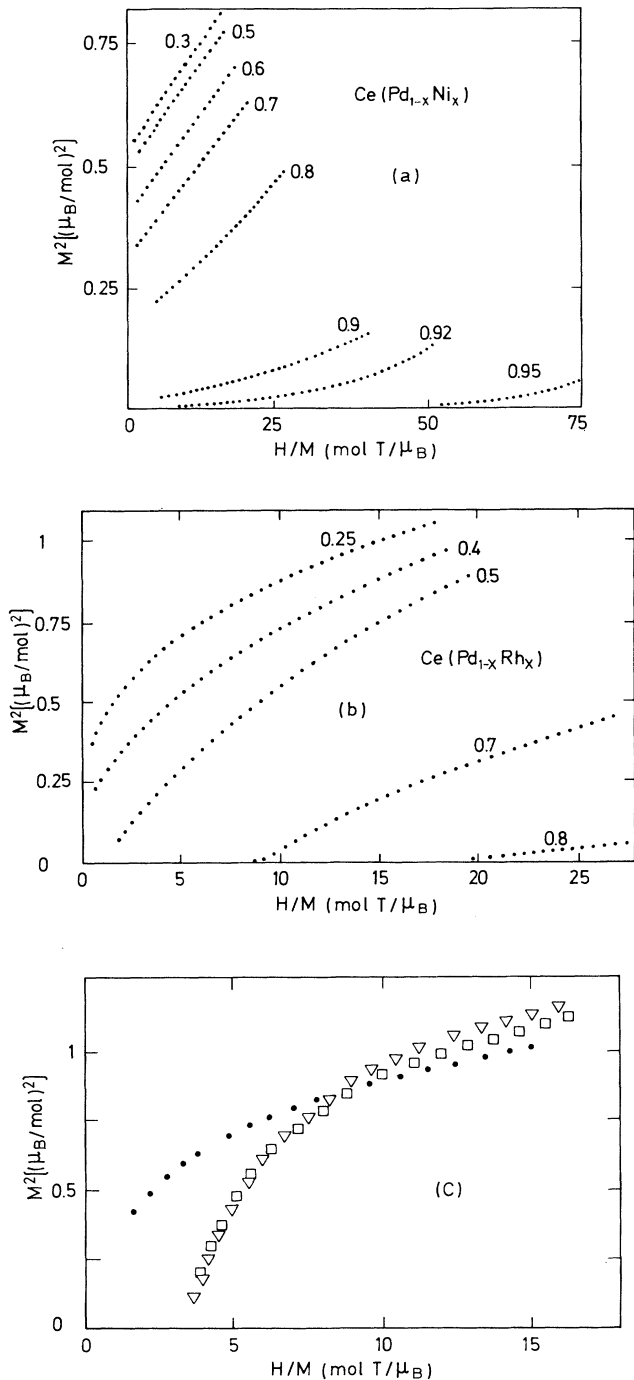


FIG. 4. Arrot plots at 4.2 K for (a) Ce(Pd_{1-x}Ni_x), (b) Ce(Pd_{1-x}Rh_x), and (c) Ce(Pd_{1-x}Ag_x) with (●) $x=0$, (□) $x=0.025$, and (▽) $x=0.10$.

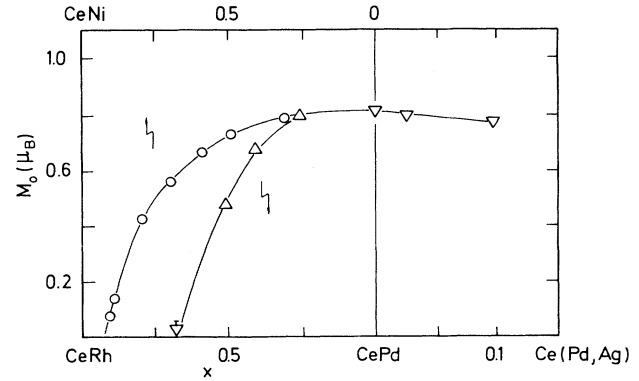


FIG. 5. Extrapolated zero-field magnetization, M_0 , at 4.2 K of Ce(Pd,Ni) (○), Ce(Pd,Rh) (△), and Ce(Pd,Ag) (▽).

quantified in terms of the expected entropy gain for a doublet GS: $\Delta S = R \ln 2$. At the ordering temperature T_C , Ce(Pd,Ni) has gained 90% of the total entropy, while Ce(Pd,Rh) only 40%. Indeed for a Ni concentration close to $x(0)$ (i.e., $x=0.9$) the $\Delta S(T)$ behavior can be compared qualitatively with that of Rh_{0.6}. The nonzero slope of $\Delta S(T)$ of Ce(Pd_{0.5}Ni_{0.5}) above T_C suggest that some hybridization effect is also present in this compound, in agreement with the $\gamma_{LT} = 21 \text{ mJ/mol K}^2$ coefficient observed at very low temperature.⁵

In the case of Ag (not shown in the figure) the $\Delta S(T)$ dependence is similar to that of the low Ni concentration. The excited crystal fields (CF's) levels are not taken into account due to the large splitting (about 200 K, Ref. 5).

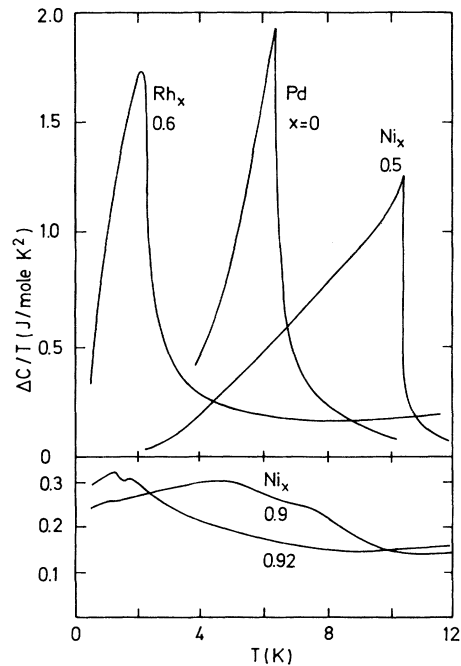


FIG. 6. Temperature dependence of the specific heat of the Ce(Pd_{1-x}M_x) compounds in a $\Delta C/T$ -vs- T plot, where ΔC denotes the phonon subtraction.

TABLE I. Magnetic, thermal, transport, and spectroscopic parameters, which characterize the $\text{Ce}(\text{Pd}_{1-x}\text{M}_x)$ compounds, $M = \text{Ni}$ and Rh .

	T_C (K)	$ \theta_p $ (K)	M_0 (μ_B)	$\Delta S(T_C)$ ($R \ln 2$)	γ (mJ/mol K^2)	$\Delta\rho_0(T_C)$ ($\mu\Omega \text{ cm}$)	$\Delta\rho_{\text{max}}$	T_{max} (K)	ν (valence)
CePd	6.6	22	0.82	~ 1	60 ^a	2	14	280	3.035
$M = \text{Ni}, x =$									
0.3	9.5		0.74						3.05
0.5	10.3	28	0.70	0.9	21	10	22	130	3.055
0.8	10.2	42	0.42			38	45	75	3.06
0.9	8.4	78	0.1	0.19	170		65	65	3.085
0.92	6.3	77	0.05	0.11	160		57	70	
1	0	200	0		60		50	120	3.10
$M = \text{Rh}, x =$									
0.25	6.0	24	0.80						3.04
0.5	4.9	26	0.47			32	30	80	3.07
0.6	2.7	37	< 0.1	0.54	177	54	44	50	3.08
0.8	0	93	0						3.125
0.85	0	180	0			40	45	70	
0.9	0	340	0			13	26	200	3.14
1	0	> 400	0		12.5	0	13	240	3.165

^aHigh temperature ($T > T_C$).

Another interesting comparison can be done between the $\Delta S(T)$ behavior of CeNi and CeRh. While in the last case a linear increase of ΔS is observed ($\Delta S = \gamma T$, with a very low value of $\gamma = 12.5 \text{ mJ/mol K}^2$, as is expected for a typical Ce-IV system with a sixfold degenerated GS, see Ref. 13), in the case of CeNi a change in the $\Delta S(T)$ slope is observed at about 40 K.¹⁴ This fact denounces CeNi as not fully IV because the CF levels are not completely degenerated. The magnetic susceptibility studies on CeNi under pressure confirm this conclusion by showing a further transition to the full IV state.¹⁵ The detailed experimental values are given in Table I.

C. Transport properties

The temperature dependence of the electrical resistivity after phonon subtraction, $\Delta\rho$, are shown in Fig. 8(a)

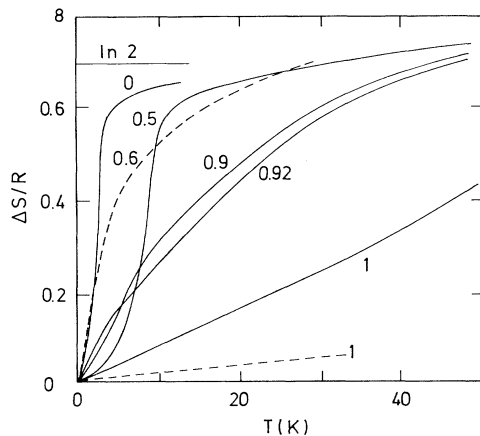


FIG. 7. Temperature dependence of the entropy gain, $\text{Ce}(\text{Pd},\text{Ni})$: continuous line and $\text{Ce}(\text{Pd},\text{Rh})$: dashed line.

for $\text{Ce}(\text{Pd}_{1-x}\text{Ni}_x)$ Ref. (5) and in Fig. 8(b) for $\text{Ce}(\text{Pd}_{1-x}\text{Rh}_x)$ (Ref. 8). The magnetic compounds CePd, Ce(Pd,Ag), and $\text{Ce}(\text{Pd}_{0.5}\text{Ni}_{0.5})$ show the characteristic drop below the ordering temperature. In $\text{Ce}(\text{Pd}_{0.5}\text{Ni}_{0.5})$, however, a maximum in $\Delta\rho$ is observed at high temperature, indicating the onset of hybridization effects on the CF excited levels. Near the $x(0)$ Ni concentration, the $\Delta\rho(T)$ slope is strongly positive at low temperature due to the dominant hybridization effect on the CF excited levels. Indeed, an unexpected linear $\Delta\rho$ vs T dependence is observed up to 25 K. On the contrary in the case of $\text{Ce}(\text{Pd},\text{Rh})$, the hybridization effects on both the GS and excited levels are put in evidence by the negative slope of $\Delta\rho(T)$ at $T \geq T_C$ and at high temperature ($T > T_{\text{max}}$, T_{max} being the temperature of $\Delta\rho_{\text{max}}$).

At the IV limit (i.e., CeNi and CeRh) a unique broad maximum is shifted to high temperatures. The comparison of the $\Delta\rho(T)$ data between $\text{Ce}(\text{Pd},\text{Ni})$ and $\text{Ce}(\text{Pd},\text{Rh})$ can be attempted by comparing some characteristic values of this parameter. We have extracted among them (see Fig. 9) (i) $\Delta\rho_0$, which is the residual paramagnetic resistivity or, eventually, $\Delta\rho(T_C)$ for those alloys that order magnetically, (ii) $\Delta\rho_{\text{max}}$, which is the maximum value of $\Delta\rho(T)$ at (iii) $T = T_{\text{max}}$, and finally (iv) T_{min} is the “relative minimum” of $\Delta\rho(T)$ between the $\Delta\rho_{\text{max}}$ due to the hybridized ground and CF excited states. Because of the intrinsic indetermination in their absolute values, these parameters (listed in Table I) have to be taken as a comparative and qualitative information.

The first difference emerging from Fig. 9, between the systems at hand, concerns the values of x at which the respective extrema of the parameters are observed. In agreement with the other physical properties, $\Delta\rho_0$, $\Delta\rho_{\text{max}}$, and T_{max} show extreme values at $x \approx 0.9$ for $\text{Ce}(\text{Pd},\text{Ni})$ and at $x \approx 0.6$ for $\text{Ce}(\text{Pd},\text{Rh})$. Other subtle differences are given by (a) the relative values of $\Delta\rho_0$ [or $\Delta\rho(T_C)$] and

$\Delta\rho_{\max}$; while in Ce(Pd,Ni) the $\Delta\rho_{\max}$ value is larger than $\Delta\rho_0$, the inverse occurs for Ce(Pd,Rh). This feature reflects the fact that in the first case there is no detectable hybridization effect on its GS, while it is significant in the second one. Note that, as the system becomes IV, for large x (Ni) values, only $\Delta\rho_{\max}$ is preserved, as the system

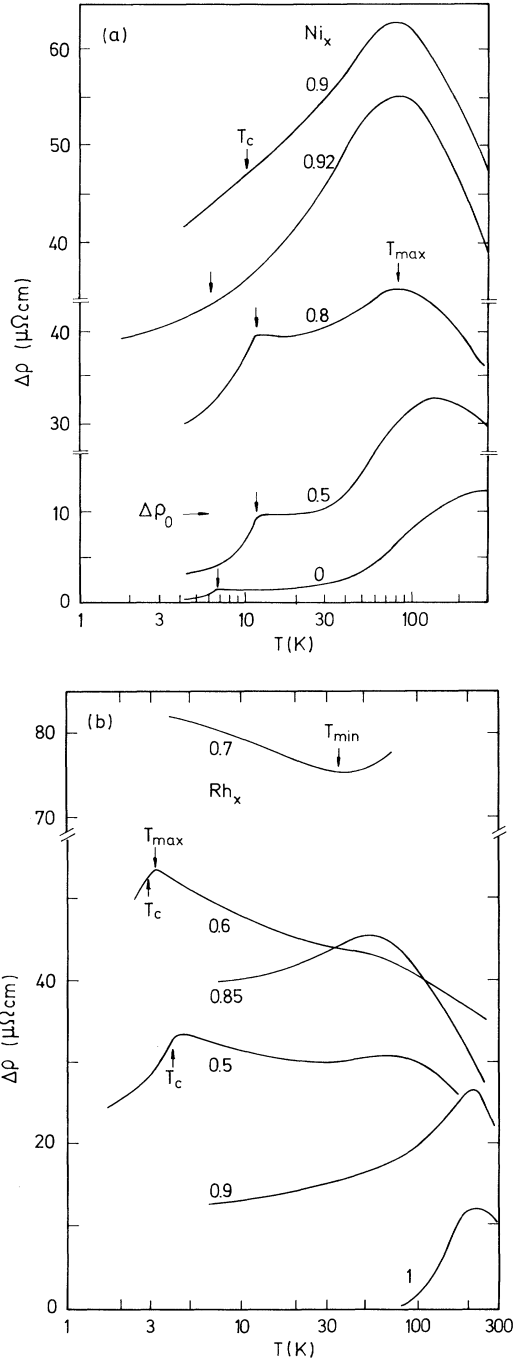


FIG. 8. (a) Temperature dependence of the electrical resistivity after phonon subtraction of Ce(Pd_{1-x}Ni_x). (b) Temperature dependence of the electrical resistivity after phonon subtraction of Ce(Pd_{1-x}Rh_x).

becomes IV. (b) T_{\min} is only observed in Ce(Pd,Rh) at intermediate x values, where the hybridization strength is still smaller than the CF splitting. The apparent absence of such hybridization of the Ce(Pd,Ni) GS avoids the $\Delta\rho(T_{\min})$ formation.

From this comparative analysis of the transport properties we can extract that here the excited CF levels show hybridization effects at any “ x ” value, while the GS behaves in a different way depending on the ΔV or ΔZ effect. In the first case (Ni substituent) the onset of the GS hybridization coincides with the mixing with the CF levels, due to the fact that the width of the excited CF level overcomes the CF splitting. In the second case (Rh substituent) the hybridization of the ground and excited levels rises independently, overlapping themselves when the system becomes IV.

D. Structural properties

The volume of the unit cell V_C changes with x as shown in Fig. 10, putting in evidence some intrinsic differences between the Ni or Rh as substituents. Though in both cases V_C decreases with x , the $V_C(x)$ dependence is essentially different. In the case of Ce(Pd,Ni), $V_C(x)$ follows the Vegard’s law up to a critical concentration (x_{cr}), above which V_C practically collapses as the hybridization strength increases. On the contrary, in Ce(Pd,Rh), $V_C(x)$ decreases faster than an estimated Vegard’s law [see the $V_C(x=1)$ extrapolation to an hypothetical Ce³⁺Rh compound in Fig. 10]. For $x > x_{cr}$ the $V_C(x)$ slope increases, but only gradually. The most striking feature comes out from that, regardless of the fact that the Ni atomic volume is 20% smaller than that of Rh, for $x < x_{cr}$ the dV_C/dx slope is smaller for Ce(Pd,Ni) than for Ce(Pd,Rh). Therefore, the obvious conclusion is that the hybridization effect is present as

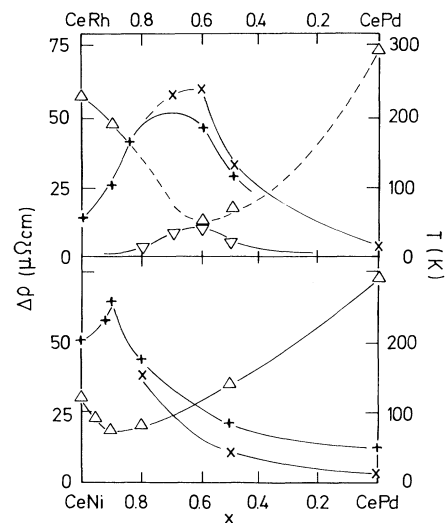


FIG. 9. Pd substitution dependence of the residual resistance $\Delta\rho_0(X)$, of the resistivity maximum $\Delta\rho_{\max}(+)$, the temperature of the maximum $T_{\max}(\Delta)$ and minimum $T_{\min}(\nabla)$ of the resistivity.

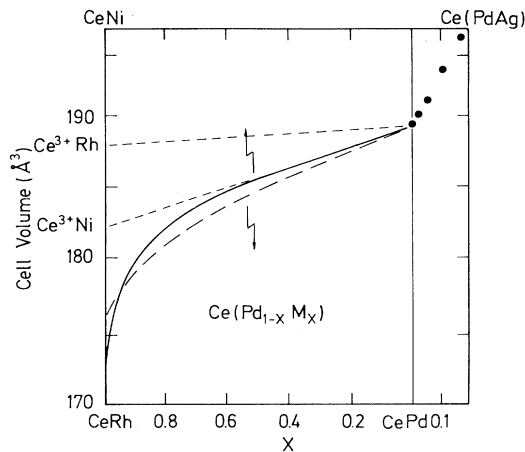


FIG. 10. Volume of the unit cell (V_c) as a function of the Pd substitution. Ce^{3+}Rh and Ce^{3+}Ni represent the calculated V_c value for those hypothetical compounds.

soon as Rh substitutes Pd, while in the case of Ni it occurs only approaching the x_{cr} value.

The $V_c(x)$ variation of $\text{Ce}(\text{Pd},\text{Ag})$ is also shown in Fig. 10. Here a Vegard-type behavior can be inferred by extrapolating $V_c(x=1)$ to four times the V_c value of the bcc-CeAg compound (notice that the unit cell of the CrB-type structure contains four formula units,¹⁶ while the CsCl one contains only one).

E. Spectroscopic measurements

The L_{III} absorption edges provide useful information about the Ce valence ν in these compounds. The L_{III} edges of CeNi and CeRh at 40 and 300 K are reported in Fig. 11 together with their thermal variation. It can be seen that the amplitude of variation of ν is small ($\Delta\nu < 0.04$) but quite significant. As discussed in Ref. 17, these variations are directly related to the characteristic energy scale of these systems, and in reasonable agreement with the one-impurity Anderson model. By comparison the Ce valence in CePd is close to 3, as expected,

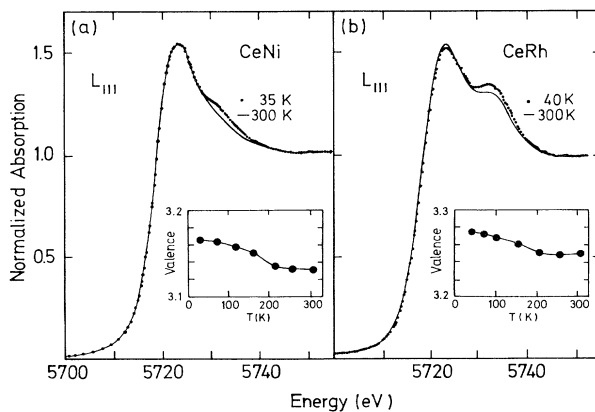


FIG. 11. L_{III} -Ce edge in (a) CeNi and (b) CeRh, at 40 and 300 K. Insets: thermal variation of the valence.

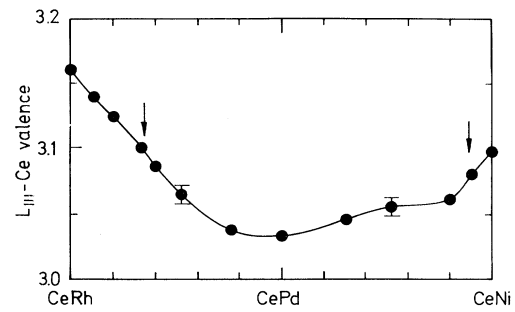


FIG. 12. Concentration variation of the valence in $\text{Ce}(\text{Pd},\text{Ni})$ and $\text{Ce}(\text{Pd},\text{Rh})$. The arrows indicate the respective critical concentrations.

and temperature independent within our resolution (± 0.02).

The comparison between the concentration variation $\nu(x)$ for $\text{Ce}(\text{Pd},\text{Ni})$ and $\text{Ce}(\text{Pd},\text{Rh})$ systems is given in Fig. 12. In agreement with the other experiments, the valence transition is more abrupt in the first case. It is remarkable that the change of slope in the $\nu(x)$ variation correlates better with the variation of Θ_p (Fig. 3), rather than with the disappearance of the magnetic order. This points out the role of hybridization effects in these systems. The $\nu(x)$ values are listed in Table I.

Important information can be obtained also from the x-ray-absorption near-edge structures (XANES) oscillations in the energy range 20–100 eV after the main line. Figure 13 shows that the $\text{CePd}_{0.5}\text{Ni}_{0.4}$ alloy still presents the characteristic XANES features of the parent compounds CeNi and CePd. It has been demonstrated that the XANES oscillations are connected with the neighbor distances (d) from the Ce atoms by taking the usual correction of the energy scale (ΔE) as a function of d : $\Delta E d^2 = \text{cte}$.¹⁸ By analogy, with these previous studies

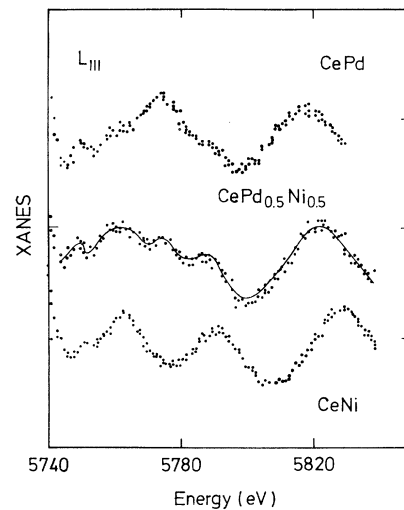


FIG. 13. XANES oscillations in the energy range of 20–100 eV after the edge for CePd, CeNi, and $\text{Ce}(\text{Pd}_{0.5}\text{Ni}_{0.5})$. See the test for the fit.

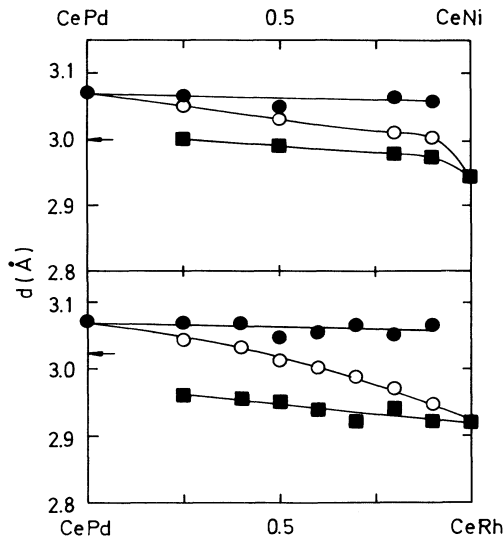


FIG. 14. Interatomic distances extracted from the XANES analysis (full symbols) and from crystallographic determination (open symbols). The arrows indicate the calculated $d(\text{Ce}^{3+}\text{-Ni})$ and $d(\text{Ce}^{3+}\text{-Rh})$.

and using the XANES spectra of CePd and CeNi (CeRh) as references, the local interatomic distances $d(\text{Ce-Pd})$ and $d(\text{Ce-Ni})$ [$d(\text{Ce-Rh})$] can be directly extracted from a fit of experimental data for the system $\text{CePd}_{1-x}\text{Ni}_x$ ($\text{CePd}_{1-x}\text{Rh}_x$). It should be noted that the Ce neighborhood in the actual crystallographic structure is rather complex and the Ce- M distances reported here represent an average on the first shells. An example of a fit is represented as a full line in Fig. 13 and the corresponding interatomic distances are reported in Fig. 14. In both cases, Ce-Pd distances remains nearly constant, suggesting that the most important part of the substitution effect is localized at the Ce- M contacts ($M = \text{Ni}$ or Rh). The two systems behave differently from this point of view: The interatomic distance $d(\text{Ce-Ni})$ in $\text{CePd}_{1-x}\text{Ni}_x$ alloys varies rapidly for $0.8 < x < 1$, in agreement with the rapid disappearance of the magnetic ground state and the evolution of lattice constant, Ce valence, etc. On the other side, when x decreases toward zero, $d(\text{Ce-Ni})$ reaches slowly the expected value for $d(\text{Ce}^{3+}\text{-Ni})$. On the other hand, in the Ce(Pd,Rh) system, $d(\text{Ce-Rh})$ varies linearly with x and extrapolates toward a value significantly lower ($\cong 0.05 \text{ \AA}$) than $d(\text{Ce}^{3+}\text{-Rh})$. This observation is in agreement with the observation that hybridization effects are already present for low Rh concentrations.

III. DISCUSSION

From these experimental results it becomes evident that the volume and the electronic concentration effects on the valence evolution of Ce are essentially different in the compounds under study. The structural pressure produced by the substitution of Pd (with a Goldschmidt atomic radius $r = 1.37 \text{ \AA}$) by a smaller atom is effective at

large Ni concentration (for Ni, $r = 1.27 \text{ \AA}$). This is due to the fact that the crystal structure is mainly supported by the large (Pd) atoms and therefore the Ce-Pd contacts are stronger than the Ce-Ni ones. Only at high Ni concentration the Ce-Ni contacts become efficient for inducing the instability in the Ce^{3+} magnetic ground state. At that point the system collapses into the IV configuration. At intermediate Ni concentration, the mean Ce-Ce distance is reduced anyway, increasing the ordering temperature, as expected for a RKKY-type interaction and, after going through a maximum, T_C decreases drastically. Within such a picture, the maximum in T_C represents the x value for which the maximum shortening of the Ce-Ce distance is reached before the Ce-Ni contacts become able to turn off efficiently the hybridization mechanism. Noteworthy is the fact that from resistivity measurements the GS appears not to be affected by the hybridization, while the excited CF levels show such effect.

On the other hand, the “electronic concentration” changes produced by Rh (with $r = 1.34 \text{ \AA}$) immediately induce hybridization effects in the ground and CF excited states. The Ce(Pd,Rh) system looks more homogeneous from the structural point of view, because (due to the similar Pd and Rh size) both Ce-Pd and Ce-Rh contacts are equally possible. Here the shortening of the Ce-Ce distance is not due to the difference in size of the Ce ligand but to the actual reduction of the Ce volume itself because of the valence increase. Such a reduction of the Ce volume is connected with the hybridization of the Ce-GS, which has started already with low Rh concentration, and therefore no maximum in T_C is expected in the whole range of substitution.

As quoted in the introduction, Ce(Pd,Ni) and Ce(Pd,Rh) have the same “matrix” compound: CePd, but their respective behaviors are qualitatively different depending on the driving parameter, ΔV or ΔZ , one concludes that $|\delta J|$ cannot be taken as a “universal” parameter for comparing different systems.

Concerning the hybridization effects on the CF excited levels in Ce(Pd,Rh), the $\Delta\rho(T)$ dependence shows that ground and excited levels are simultaneously affected. At present, we do not have an explanation for such a different behavior between the Ni and Rh compounds, but it is clear that the hybridization strength is different for different self-states and therefore for different symmetries.

Finally, we attempt to check empirically the exponential dependence of T_K with $|\delta J|$. By taking T_K as proportional to $|\theta_p|$,¹⁹ and neglecting CF effects, we have plotted, in Fig. 15, the $\ln|\theta_p|$ experimental values of Ce(Pd,Ni), Ce(Pd,Rh), and Ce(Pt,Ni) (extracted from Ref. 4) vs the inverse of the concentration, defined as $(x_0 - x)^{-1}$, simulating the T_K vs $\exp(-1/|\delta J|)$ equation. The only adjustable parameter is x_0 , which has the same value for the Pd-Ni and Pt-Ni substitution: $x_0 = 1.15$ and 1.03 for Pd-Rh. We have to note that the x_0 value is critical for $x \rightarrow 1$, but the coincidence shown in Fig. 15 shows the validity of the proposed functionality. The oscillations around the straight line are probably due to the CF levels population, which are affected by their own hybridization strength.

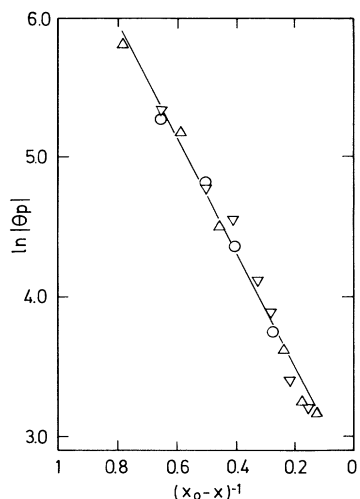


FIG. 15. Exponential dependence of $|\theta_p|$ on $(x_0-x)^{-1}$, see the text, for Pd substitution by Ni (\circ), Rh (\triangle), and Pt by Ni (∇).

IV. CONCLUSIONS

From this comparative study on the $\text{Ce}(\text{Pd}_{1-x}\text{M}_x)$ family of compounds we can conclude the following.

(i) A maximum in $T_0 = f(|\delta J|)$ is observed when there is a range of substitution in which the eventual (weak) hybridization strength does not affect the intensity of the GS magnetic moment. In other words, there is a threshold value (at $|\delta J|_{\text{max}}$) for the hybridization below which the GS magnetic properties are not affected.

(ii) ΔV and ΔZ are not equivalent as applied "chemical pressure" parameters because the first one implies different Ce-ligand spacings in different space directions

(inhomogeneity), while the crystal structure is supported by the larger partner, and the second one induces a continuous (and homogeneous) change in the chemical potential.

(iii) It is possible to distinguish between the Ce-Ce spacing reduction originated in the ΔV of the Ce-ligand (Vegard's law) and in the Ce-volume decrease related to its change of valence.

(iv) Concerning the comparison between the effect of the Ce-ligand substitution by a holelike atom (Pd substitution by Rh and Ni) or by an electronlike one (Ag), it is clear that the local change of the sign of the electronic charge of the partner breaks the spatial charge periodicity, transforming the magnetic structure of the system. This effect was confirmed by further Pd substitutions such as by the holelike Co, Ir, and Pt, which keep the ferromagnetic behavior. On the other hand, the electronlike Cu and Au transform to an antiferromagnetic behavior.¹¹

(v) It is possible to distinguish between different hybridization strengths on the GS and the CF-excited states. However, the existence of a strongly hybridized magnetic GS in $\text{CePd}_{1-x}\text{Rh}_x$ in the $0.4 < x < 0.65$ range remains an interesting problem.

These conclusions should be confirmed by similar studies on other Ce-ligand substituted systems before taking them as general features. With such a purpose a wider study including most of the known Ce systems is in progress.

ACKNOWLEDGMENTS

One of us (J.G.S.) wishes to thank the Alexander von Humboldt Foundation of Germany and the Fundacion Antorchas of Argentina for their support.

¹S. Doniach, *Physica C* **91B**, 231 (1977).

²F. Steglich, *J. Magn. Magn. Mater.* **100**, 186 (1991).

³S. M. Evans, A. K. Bhattacharjee, and B. Coqblin, *Physica B* **171**, 297 (1991).

⁴D. Gignoux and J. C. Gomez-Sal, *Phys. Rev. B* **30**, 3967 (1984).

⁵G. L. Nieva, J. G. Sereni, M. Afyouni, G. Schmerber, and J. P. Kappler, *Z. Phys. B* **70**, 181 (1988).

⁶R. Lahiouel, R. M. Galera, J. Pierre, and E. Siaud, *Solid State Commun.* **58**, 815 (1986).

⁷A. Eiling and J. S. Schilling, *Phys. Rev. Lett.* **46**, 364 (1981).

⁸J. P. Kappler, E. Beaurepaire, G. Krill, C. Godart, G. Nieva, and J. G. Sereni, *J. Phys. (Paris) Colloq.* **49**, C8-723 (1988); and J. P. Kappler, M. J. Besnus, A. Herr, A. Meyer, and J. G. Sereni, *Physica B* **171**, 346 (1991).

⁹J. Lawrence, *Phys. Rev. B* **20**, 3770 (1979).

¹⁰W. H. Lee, R. N. Shelton, S. K. Dahr, and K. A. Gschneidner, Jr., *Phys. Rev. B* **35**, 8523 (1987).

¹¹J. P. Kappler, G. Schmerber, and J. G. Sereni, *J. Magn. Magn. Matter.* **76-77**, 185 (1988).

¹²J. G. Sereni and J. P. Kappler (unpublished).

¹³J. G. Sereni, *Handbook on the Physics and Chemistry of Rare Earths*, edited by K. A. Gschneidner, Jr. and L. Eyring (Elsevier Science, British Vancouver, 1991), Vol. 15, Chap. 98, p. 1.

¹⁴The $\Delta S(T)$ dependence was extracted from the $C_p(T)$ measurements from D. Gignoux, F. Givord, and R. Lemaire, *J. Less-Common Met.* **94**, 165 (1983).

¹⁵D. Gignoux, C. Vettier, and J. Vioron, *J. Magn. Magn. Mater.* **70**, 388 (1987).

¹⁶See, for example, O. Schob and E. Parth, *Acta Cryst.* **19**, 214 (1965).

¹⁷E. Beaurepaire, J. P. Kappler, J. G. Sereni, C. Godart, and G. Krill, in *X-ray Absorption Fine Structure, Proceedings of the XAFS VI, York, 1990*, edited by S. Hashain (Ellis Horwood, York, U.K., 1991), p. 505.

¹⁸C. R. Natoli, in *EXAFS and Near Edge Structure*, edited by A. Bianconi, L. Incoccia, and S. Stipcich (Springer-Verlag, Berlin, 1983), p. 43.

¹⁹Krishna-murthy, K. G. Wilson, and J. W. Wilkins, *Phys. Rev. Lett.* **35**, 1101 (1975).